Volume 14
Number 6
June 2023
Pages 995–1200

# RSC Medicinal Chemistry

rsc.li/medchem

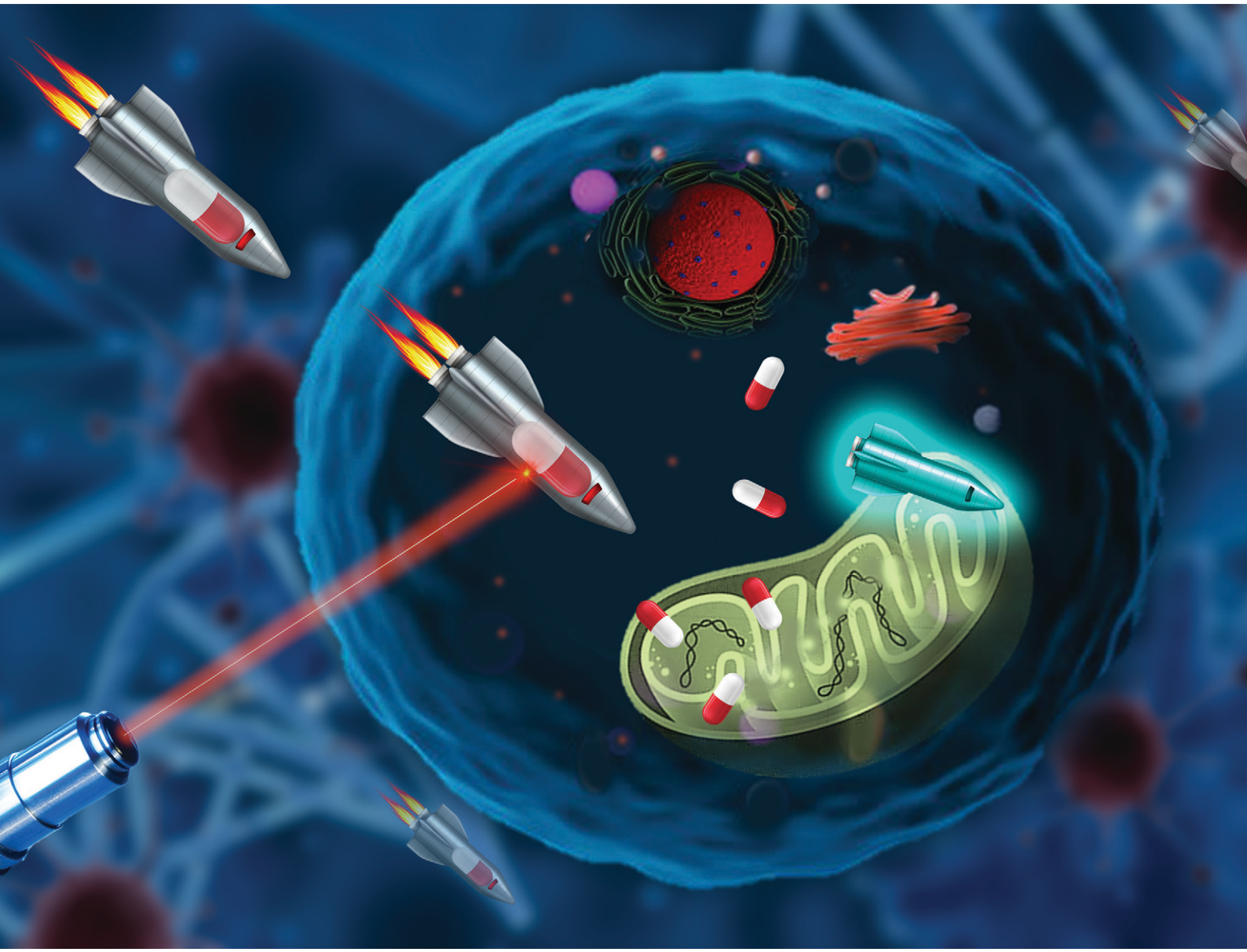

ISSN 2632-8682

ROYAL SOCIETY OF CHEMISTRY

**RESEARCH ARTICLE**
Pijus K. Sasmal *et al.*
Visible and NIR light photoactivatable *o*-hydroxycinnamate system for efficient drug release with fluorescence monitoring

RSC Medicinal Chemistry

ROYAL SOCIETY OF CHEMISTRY

RESEARCH ARTICLE



Cite this: *RSC Med. Chem.*, 2023, **14**, 1088

# Visible and NIR light photoactivatable *o*-hydroxycinnamate system for efficient drug release with fluorescence monitoring†

Ajay Gupta,[a] Neelu Singh,[a] Aryan Gautam,[a] Neetesh Dhakar,[b] Sunil Kumar [b] and Pijus K. Sasmal *[a]

Received 14th December 2022,
Accepted 28th February 2023

DOI: 10.1039/d2md00438k

rsc.li/medchem

Photoactivatable protecting groups (PPGs) have become powerful materials for controlling the activity of biologically important molecules in the biomedical field. However, designing PPGs that can be efficiently activated by biologically benign visible and NIR light with fluorescence monitoring is still a great challenge. Herein, we report *o*-hydroxycinnamate-based PPGs that can be activated by both visible (one-photon) and NIR (two-photon) light for controlled drug release with real-time monitoring. Thus, a photoremovable 7-diethylamino *o*-hydroxycinnamate group is covalently attached to an anticancer drug, gemcitabine, to establish a photoactivatable prodrug system. Upon excitation by visible (400–700 nm) or NIR (800 nm) light, the prodrug efficiently releases drug which is quantified by monitoring the formation of a strongly fluorescent coumarin reporter. The prodrug is taken up by the cancer cells and interestingly accumulates within mitochondria as determined by FACS and fluorescence microscopy imaging. Further, the prodrug demonstrates photo-triggered, dose-dependent, and temporally controlled cell death upon irradiation with both visible and NIR light. This photoactivatable system could be useful and adapted in the future for the development of advanced therapies in biomedicine.

## Introduction

Controlling the activity of biologically important compounds with light is a constantly growing concern and has gained immense interest in chemical biology and medicinal chemistry.[1–4] Light has the power to manipulate biological processes in living systems with high spatial and temporal precision. In this regard, photolabile (also commonly termed as photoactivatable, photoremovable, photoreleasable, or photocleavable) protecting groups (PPGs) or photocaged compounds (PCs) have received enormous attention for the controlled release of biological effector molecules to induce biochemical function.[6–11] These compounds can be conjugated with effector molecules to mask their biological functions. The biological activities of such molecules can be restored upon removal of these photoactivatable groups by irradiation with a suitable wavelength of light. To date, various PPGs or PCs have been developed based on *o*-nitrobenzyl,[7–14] coumarinyl,[5,7–11,15–17] anthracenyl,[7–10,18,19] quinolinyl,[7–10,20,21] *p*-hydroxyphenacyl,[7–10,22] *o*-hydroxycinnamate,[8–10,23–27] rhodamine,[10,28] cyanine,[8,10,11,29] BODIPY,[8,10,11,30] *etc.* These compounds are successfully used for non-invasive spatiotemporal control over the release of biologically important compounds such as anticancer agents, antibiotics, biomolecules, neurotransmitters, fragrances, fluorescent probes, *etc.* However, most of these PPGs or PCs require high-energy UV light for their removal, which limits their biological and medical applications, since UV light is harmful to biomatter and has a quite narrow penetration potential in human tissues.[8,10,16,23] Therefore, the development of new PPGs that can be efficiently activated by biologically and chemically benign visible and near-infrared (NIR) light is highly desired to achieve deeper tissue penetration and to diminish phototoxicity.

In recent years, *o*-hydroxycinnamate (*o*HC)-based photocaged systems have received ample attention because of their (i) ease of synthesis, (ii) clean and rapid photo-uncaging capability, (iii) applicability for two-photon uncaging efficiencies by NIR light irradiation, (iv) facile conjugation with alcohols and amines without forming a carbonate bond, which is highly labile in physiological conditions, and (v) resulting photoproduct coumarin derivatives which are strongly fluorescent that served as a fluorescent reporter for the real-time monitoring of the

[a] *School of Physical Sciences, Jawaharlal Nehru University, New Delhi 110067, India. E-mail: pijus@mail.jnu.ac.in*
[b] *Department of Physics, Indian Institute of Technology Delhi, New Delhi 110016, India*

† Electronic supplementary information (ESI) available Methods, relevant experimental procedures, characterization data, cytotoxicity studies, figures and table. See DOI: **https://doi.org/10.1039/d2md00438k**

release of substrates.[23,26] The photo-uncaging capabilities of the *o*HC systems were first described by Porter *et al.* to accomplish photochemical activation of serine proteinase enzymes.[24,31,32] Jullien *et al.* have utilized the photo-triggering ability of *o*HC for the release of caged substrates such as alcohol in real-time by monitoring the formation of fluorescent coumarin reporter by irradiation with two-photon light.[25,33,34] Singh and co-workers have developed a fluorescent version of *o*HC by attaching it to an excited-state intramolecular proton transfer (ESIPT) moiety to achieve image-guided delivery of the caged substrate in biological systems and also to monitor the photo-triggered release of the caged substrate in real-time.[26] Recently, this group has demonstrated another efficient photoactivatable system based on a carbazole-fused *o*HC platform for the dual uncaging of alcohols (same or different) upon one- and two-photon irradiation with real-time monitoring capability.[35] Zhang and Wang's group first demonstrated temporally controlled anticancer drug release using an *o*HC system where the drug release was sequentially triggered by internal stimulus with nitroreductase followed by external stimulus with UV light.[36] However, the above system releases drug upon UV light irradiation which is not suitable for therapeutic applications. To address this, recently our group has made an effort to develop an organelle-targeted *o*HC-based photoactivatable drug delivery system, wherein the drug release was achieved by both UV (one-photon) or biologically benign NIR (two-photon) light irradiation with fluorescence monitoring.[37] Although this system can be activated by NIR light, poor drug release capability (32% drug release after 22 min irradiation) was observed that results in lower photocytotoxicity. Moreover, the released coumarin product is inapplicable for *in vivo* bioimaging since it emits at the UV region ($\lambda_{em}$ = 385 nm). Hence, the design of new *o*HC-based photoactivatable prodrug systems that can be efficiently activated by NIR light and are capable of performing real-time bioimaging in the visible region along with high NIR photocytotoxicity is highly desirable for potential biomedical applications.

In this study, we have designed a photoactivatable *o*HC prodrug which showed efficient and temporally controlled drug release upon visible and NIR light irradiation (Scheme 1). In our design strategy, the photoactivatable *o*HC was conjugated with an anticancer drug, gemcitabine (**GMC**), to establish the ***o*HC-GMC** prodrug. The prodrug was efficiently activated by both visible (400–700 nm) and NIR

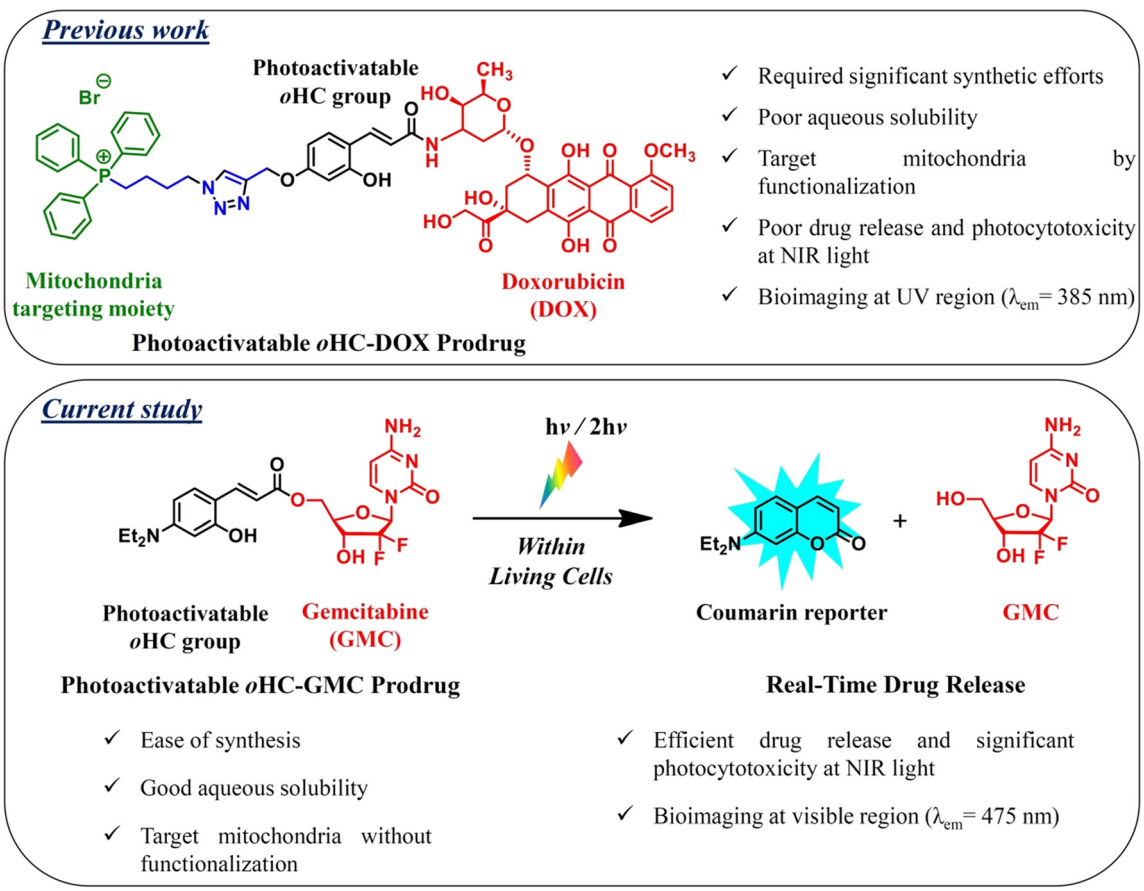


**Scheme 1** Previous work[37] and current study on a photoactivatable *o*-hydroxycinnamate-doxorubicin/gemcitabine (**oHC-DOX/GMC**) prodrug which upon irradiation with UV/visible (one-photon) or NIR (two-photon) light releases anticancer drug (**DOX/GMC**) with real-time monitoring by the formation of fluorescent coumarin reporter in living cells.

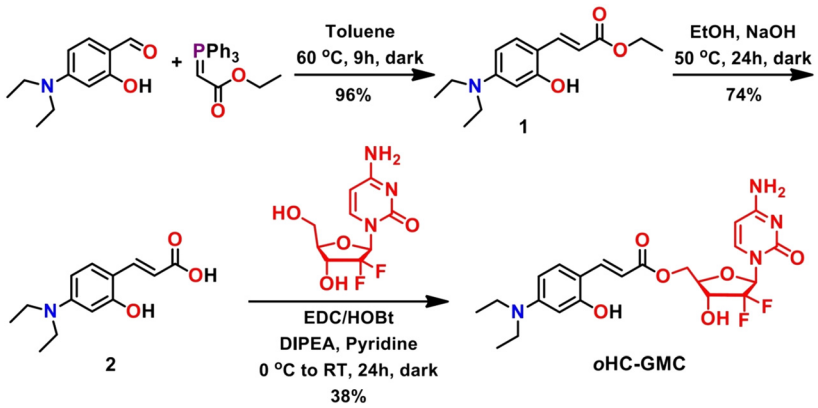


Scheme 2 Synthesis of *o*-hydroxycinnamate–gemcitabine (**oHC-GMC**) prodrug.

(800 nm) light, showing drug release of 89% and 77% with 20 min and 11 min irradiation, respectively. The release of drug can be monitored by the formation of the strongly fluorescent coumarin reporter that emits at the visible region which is appropriate for bioimaging applications ($\lambda_{em}$ = 475 nm). Interestingly, our ***o*HC-GMC** prodrug preferentially internalized in the mitochondria of cancer cells and demonstrated light-triggered temporally controlled drug release which can be observed by fluorescence microscopy imaging. Further, the prodrug exhibited dose-dependent and temporally controlled cell death upon irradiation with visible or NIR light, while negligible cell death was observed in the absence of light.

## Results and discussion

### Synthesis and photophysical properties of *o*HC-GMC

In order to achieve efficient drug release under visible and NIR light, we have synthesized a photoactivatable *o*HC-based prodrug system. For this, the photoremovable 4-(diethylamino)-2-hydroxycinnamic acid (*o*HC) was covalently conjugated with a model anticancer drug gemcitabine (**GMC**) to establish ***o*HC-GMC** (Scheme 2). Briefly, commercially available 4-(diethylamino)-2-hydroxybenzaldehyde was reacted with carboethoxymethylidenetriphenylphosphorane by the Wittig reaction to obtain the photoactivatable 4-(diethylamino)-2-hydroxy-*trans*-cinnamic ester (**1**) and its subsequent hydrolysis yielded 4-(diethylamino)-2-hydroxy-*trans*-cinnamic acid (**2**). An EDC/HOBt coupling of the carboxylic acid group of compound **2** with **GMC** provided a photoactivatable ***o*HC-GMC** prodrug. All the compounds were synthesized in a straightforward way and were easy to purify.

The photophysical properties of compound **2** and ***o*HC-GMC** were studied in 10% DMSO in phosphate buffer (100 mM, pH 7.3). Compound **2** showed absorption bands at 263 nm and 359 nm, while ***o*HC-GMC** showed bands at 266 nm and 380 nm (Fig. 1, S1 and Table S1†). The shifting of the band from 359 nm in **2** to 380 nm in ***o*HC-GMC** suggested the conjugation of compound **2** to **GMC**. The absorption band that appeared at 380 nm in ***o*HC-GMC** was used for photoexcitation. Notably, the tail of this absorption band extends beyond 500 nm into the visible region which has been utilized for its photoexcitation by visible light. Interestingly, the photoproduct coumarin compound of ***o*HC-GMC** exhibited an emission at 475 nm which is appropriate for bioimaging applications as compared to that in a previous report with an emission of 385 nm (ref. 37) (Fig. 1).

### Photo-triggered drug release properties of *o*HC-GMC

The photo-triggered drug (**GMC**) release by ***o*HC-GMC** was studied by spectroscopic techniques such as absorption and emission spectroscopy and high performance liquid chromatography (HPLC). For this, ***o*HC-GMC** solution was irradiated with visible light (400–700 nm, 11 mW) for 0–20 min and the release of **GMC** was monitored by absorption spectroscopy. The absorbance of ***o*HC-GMC** was found to gradually decrease with increasing photoirradiation time and become saturated after 20 min (Fig. 2a). Further, the drug release by ***o*HC-GMC** was also examined by emission spectroscopy by recording the emission spectra of the coumarin reporter ($\lambda_{ex}$ = 385 nm) after irradiation with visible light for 0–20 min (see Scheme 1 and Fig. 2b and c). The

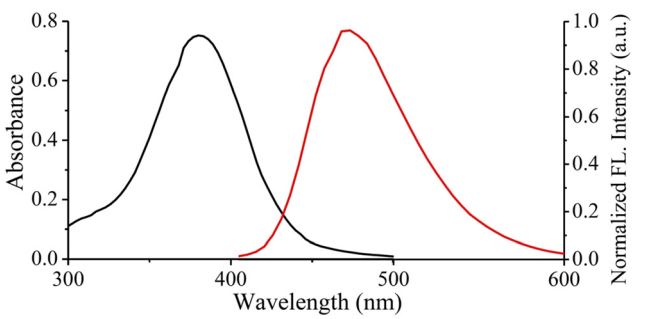


Fig. 1 Absorbance spectrum (black) of the lowest-energy absorption band of **oHC-GMC** (10 μM) and emission spectrum (red) for the photoproduct coumarin compound of **oHC-GMC** (50 μM) in 1 : 9 DMSO and phosphate buffer (100 mM, pH 7.3) at 25 °C. The emission spectrum was recorded at an excitation wavelength of 385 nm ($\lambda_{em}$ = 475 nm).

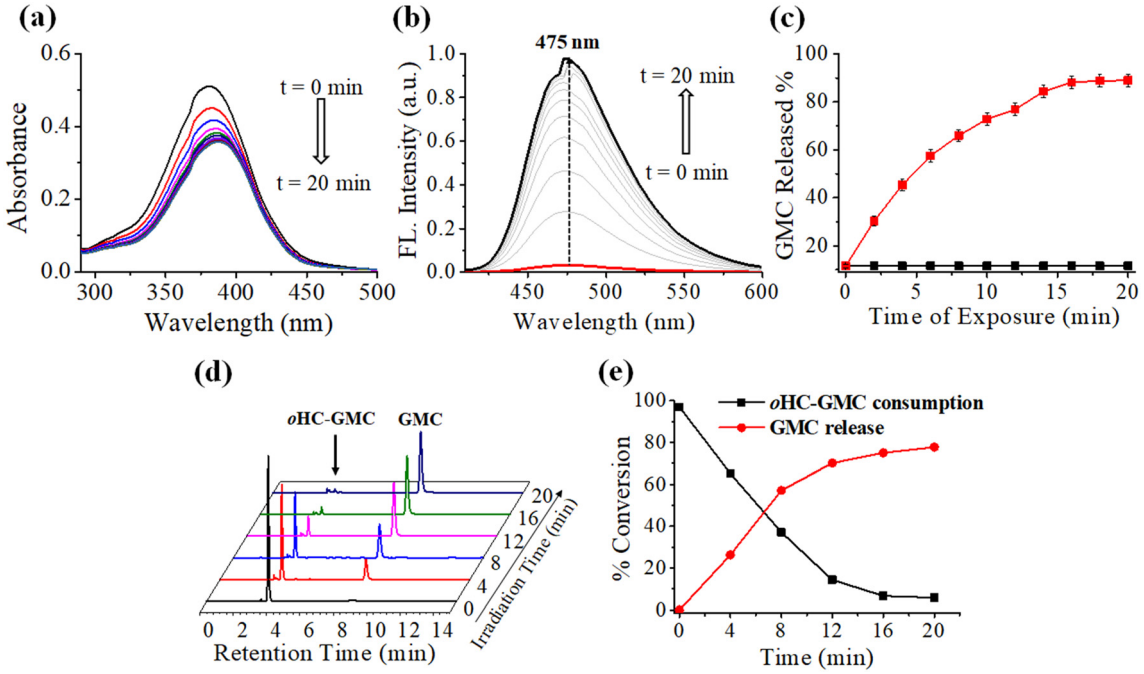


**Fig. 2** (a) Absorption and (b) emission spectra of ***o*HC-GMC** in 1 : 9 DMSO/PBS (100 mM, pH 7.3) upon irradiation with visible light (400–700 nm, 11 mW) at 25 °C. Each time the sample was exposed to light for 2 min before measuring the absorption and emission spectra. The emission ($\lambda_{ex}$ = 385 nm) spectra of ***o*HC-GMC** before (red line) and after 20 min irradiation (black line) are highlighted. (c) Kinetic curve at $\lambda_{em}$ 475 nm for the release of **GMC** from ***o*HC-GMC** in the dark (■) or under light (■) irradiation. (d) HPLC monitoring of the progress of the release of **GMC** from ***o*HC-GMC** in 1 : 9 MeCN/PBS (100 mM, pH 7.3) under visible light (400–700 nm, 11 mW) irradiation at 25 °C. (e) Quantitative monitoring of the conversion of ***o*HC-GMC** (50 μM) to **GMC** in 1 : 9 MeCN/PBS (100 mM, pH 7.3) at 25 °C under visible light irradiation.

results showed that the emission intensity of coumarin reporter at 475 nm gradually increased and was eventually saturated at 20 min photoirradiation. The drug release determined by emission spectroscopy upon photoirradiation was found to be 89%. However, there was no change in emission spectra observed without photoirradiation, suggesting that the coumarin product was not formed, which implied no drug release. Hence, our photo-triggered ***o*HC-GMC** system showed controlled drug release with real-time monitoring by measuring the fluorescence intensity of the formed coumarin product. In addition, the drug release was also evaluated by monitoring the photochemical conversion from ***o*HC-GMC** to **GMC** using RP-HPLC (Fig. 2d and e). Before photoirradiation, a single peak of ***o*HC-GMC** was observed in the HPLC chromatogram at a retention time of 3.7 min. However, the intensity of the peak at 3.7 min gradually decreased upon photoirradiation, whereas a new peak was developed at 8.9 min corresponding to **GMC**. The HPLC results suggested 78% conversion of ***o*HC-GMC** to **GMC** upon 20 min exposure to visible light. In general, the ***o*HC-GMC** prodrug undergoes *trans*-to-*cis* photoisomerization followed by lactonization to form a fluorescent coumarin product, thereby facilitating the release of **GMC**.[23,33,37]

Next, we determined the uncaging quantum yields of ***o*HC-GMC** upon irradiation with visible light. The uncaging quantum yield ($\Phi_u$) of *E*-to-*Z* photoisomerization of ***o*HC-GMC** after one-photon excitation with visible light was determined to be 0.028 (±0.007%), which is comparable to that of other reported *o*HC-based systems wherein the photo-uncaging studies were performed under UV light (Table S1†).[33–35]

We also investigated the effect of pH on the drug release profile from ***o*HC-GMC** after irradiation with visible light in order to determine its potential application in biological medium (Fig. S2†). Thus, drug release studies were carried out over a wide pH range of 4–9 and the release of **GMC** was determined by measuring the fluorescence intensity of coumarin product after photoirradiation. It was observed that the drug release is pH-dependent, which increased with the increase in pH. The maximum drug release was determined between pH 7 and 9. In contrast, very little drug release was observed under acidic conditions at pH 4, which is in accordance with the literature.[27] Hence, our ***o*HC-GMC** system is suitable for drug release studies under physiological pH conditions (pH 7.3), where the drug release was found to be maximum.

## Cellular uptake and photo-triggered *in vitro* drug release of *o*HC-GMC

Before determining the cellular uptake, the lipophilicity (log $P_{o/w}$) of ***o*HC-GMC** was determined by measuring its partition coefficient in an *n*-octanol/water system.[37,38] The log $P_{o/w}$ value of ***o*HC-GMC** was found to be 2.1, suggesting its moderately lipophilic nature (Table S1†). Then, we investigated the uptake of ***o*HC-GMC** in human lung

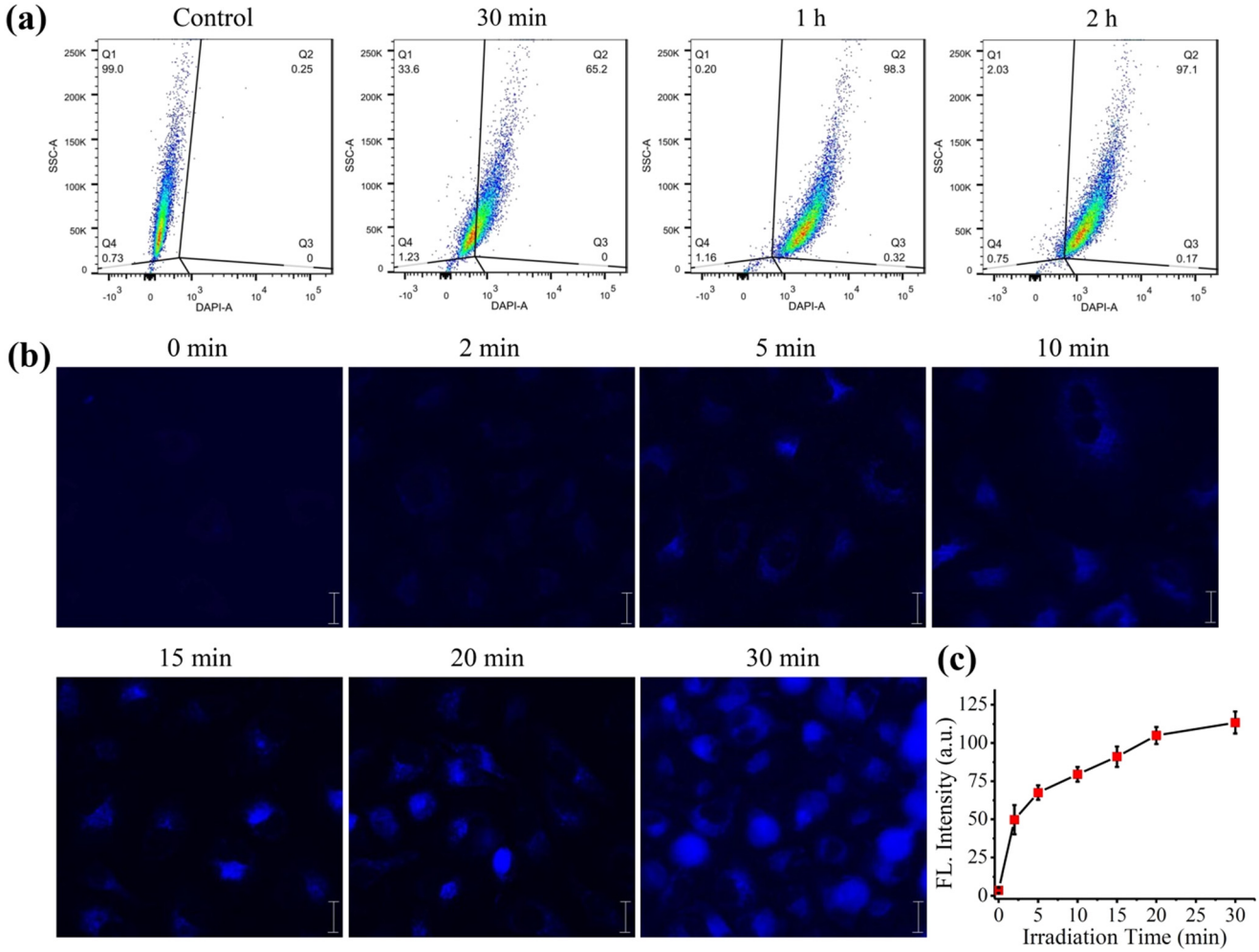


**Fig. 3** (a) Uptake of ***o*HC-GMC** (10 μM) in A549 cells at different incubation time points (30 min, 1 h, and 2 h) determined by FACS analysis. The control represents untreated cells. (b) Monitoring the intracellular drug release by ***o*HC-GMC** (10 μM) in A549 cells upon photoexposure to visible light (400–700 nm, 11 mW) for different time points by measuring the blue fluorescence intensity of the photoproduct coumarin compound determined by fluorescence microscopy imaging. Scale bar = 20 μm. (c) The graph represents the drug release as a function of irradiation time from ***o*HC-GMC** (10 μM) in A549 cells by measuring the fluorescence intensity of the photoproduct coumarin corresponding to the fluorescence images shown in (b).

carcinoma (A549) cells at different time points using fluorescence-activated cell sorting (FACS) analysis (Fig. 3a). The maximum uptake of prodrug was found at 1 h.

Next, we evaluated and monitored the photo-triggered drug release by ***o*HC-GMC** in cancer cells by fluorescence microscopy imaging (Fig. 3b). For this, the cultured A549 cells were incubated with 10 μM concentration of ***o*HC-GMC** at 37 °C for 1 h, washed with PBS followed by irradiation with visible light (400–700 nm, 11 mW) for 0, 2, 5, 10, 15, 20, and 30 min and further incubated at 37 °C for 10 min before fluorescence imaging. Upon irradiation with light for 2 min, a very weak blue fluorescence was developed and the intensity of the blue fluorescence increased with increasing exposure time (Fig. 3c). These results indicated that the drug release can be modulated by varying the exposure time to light that can be simply monitored by measuring the fluorescence intensity of the coumarin reporter in living cells, providing real-time monitoring of temporally controlled drug release.

## Subcellular localization studies

To investigate the subcellular localization of ***o*HC-GMC**, we performed a co-localization study using organelle staining dye by fluorescence microscopy imaging. Accordingly, the cells were incubated with ***o*HC-GMC** (10 μM) and then irradiated with visible light for 10 min, followed by incubation with mitochondrial (Mito Red, 100 nM) staining dye (Fig. 4a). The overlap of the blue fluorescence intensity of the photoproduct coumarin reporter (Fig. 4a(A)) with the red fluorescence of Mito Red dye (Fig. 4a(B)) appeared as a pink color (Fig. 4a(C)). Further, the degree of co-localization was also determined using a scatter plot which showed 59% overlap of the blue and red signals (Fig. 4a(D)). The results suggested that the released photoproduct fluorescent coumarin reporter, *i.e.*, 7-diethylamino coumarin (see Scheme 1), accumulated in the mitochondria of cancer cells, which is well supported by literature reports.[39,40] However,

 

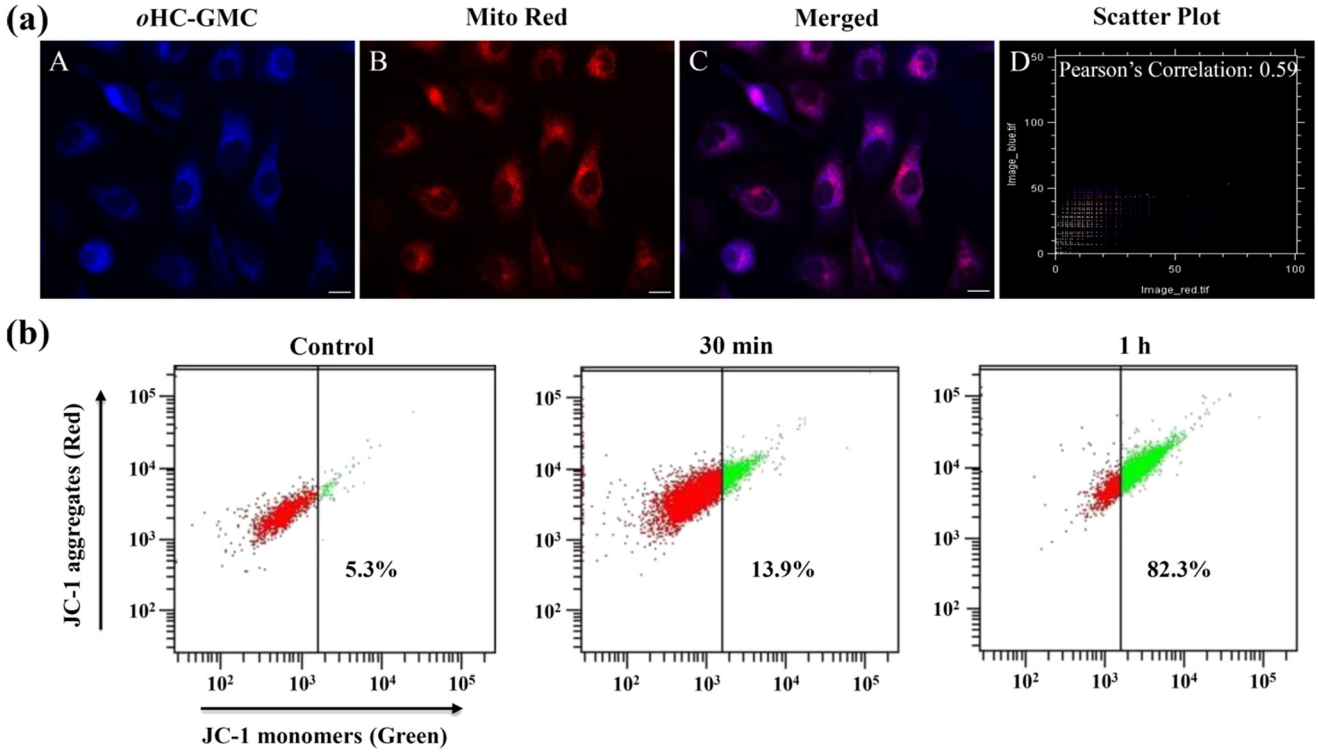


**Fig. 4** (a) Subcellular localization of the photoproduct coumarin compound of ***o*HC-GMC** in A549 cells examined by fluorescence microscopy. A549 cells treated with ***o*HC-GMC** (10 μM) followed by photolysis with visible light (400–700 nm, 11 mW) for 10 min: (A) fluorescence image of formed coumarin product after photolysis of ***o*HC-GMC** ($\lambda_{ex}/\lambda_{em}$ = 350/460 nm), (B) mitochondrial staining with Mito Red dye ($\lambda_{ex}/\lambda_{em}$ = 550/580 nm), (C) upon merging of images A and B, and (D) scatter plot representing the extent of co-localization. Scale bar = 20 μm. (b) Effects of ***o*HC-GMC** (10 μM) on MMP analyzed by FACS analysis. A549 cells were treated for 30 min and 1 h, then stained with JC-1 dye.

we cannot conclude that the photo-uncaging reaction or the coumarin release took place in the mitochondria. The photo-uncaging can occur within the cytoplasm followed by the diffusion of the photoproduct coumarin compound to the mitochondria. In order to examine whether the photo-uncaging reaction happened within the mitochondria, we checked the subcellular localization of the ***o*HC-GMC** prodrug in the cells prior to photoirradiation. The accumulation of prodrug within mitochondria will lead to a change in the mitochondrial membrane potential (MMP), designated by $\Delta\Psi_m$. To determine the change in the MMP, we used JC-1, a membrane-permeable mitochondria-selective dye which emits red and green fluorescence in its aggregate and monomeric states, respectively.[41] In a healthy polarized mitochondrion having high membrane potentials, JC-1 exists in the form of J-aggregates and emits red fluorescence, whereas in a depolarized mitochondrion having low membrane potentials, JC-1 exists in the form of a J-monomer and emits green fluorescence. The ratio of red to green fluorescence of JC-1 is frequently employed for detecting the change in the MMP. Thus, we monitored the change in $\Delta\Psi_m$ by measuring the fluorescence of JC-1 (red)/JC-1 (green) upon treatment of A549 cells with ***o*HC-GMC** (10 μM) prodrug by FACS analysis (Fig. 4b). The control cells exhibited red fluorescence, indicating that the mitochondrial membrane retains a high potential. In contrast, the cells treated with ***o*HC-GMC** showed a marked decrease in $\Delta\Psi_m$, as evidenced by the shifting of fluorescence from red to green, suggesting depolarization of mitochondria. The percentage of cells with mitochondrial membrane depolarization increased with the incubation time of ***o*HC-GMC** from 13.9 ± 1.1% at 30 min to 82.3 ± 8.5% at 1 h as compared to the control cells (5.3 ± 1.1%). The above results clearly suggested that our prodrug targets mitochondria without its functionalization with the mitochondria-targeting moiety. This result is also further corroborated by co-localization studies which revealed that upon photoexposure to ***o*HC-GMC**, the photoproduct coumarin compound accumulated in the mitochondria of cancer cells (Fig. 4a). The uptake of ***o*HC-GMC** prodrug into cells possibly takes place through a diffusion mechanism.[40] The lipophilic nature of our prodrug and its depolarizing effects on mitochondria could be the cause of its accumulation within mitochondria.[39,42–44] Recently, mitochondria-targeted drug delivery systems have gained considerable interest since the mitochondrial dysfunction is responsible for a variety of human diseases including cancer and it also plays a pivotal role in cell death by initiating apoptosis, which is regarded as a major mode of cell death in cancer therapy.[45,46] Hence, our designed prodrug could be a promising candidate for the effective treatment of cancer.

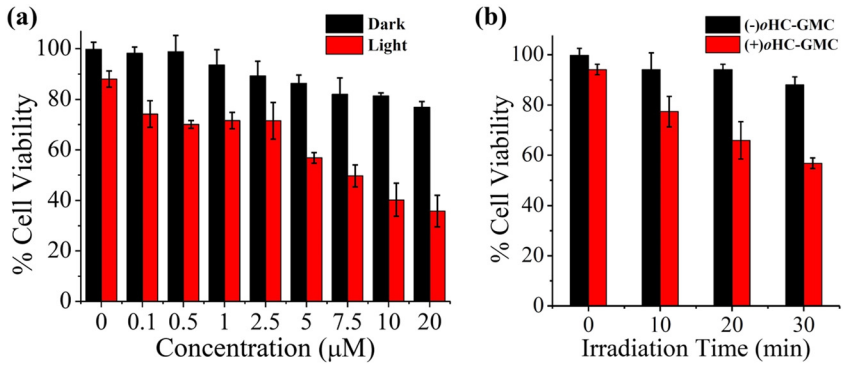


**Fig. 5** Cell viability as determined by MTT assay in A549 cells treated (a) with different concentrations of ***o*HC-GMC** prodrug in the absence (black bar) or presence (red bar) of visible light (400–700 nm, 11 mW) for 30 min of irradiation and (b) without (–) or with (+) the ***o*HC-GMC** prodrug (5 μM) by varying the exposure time of light irradiation.

### Visible-light-induced photocytotoxicity of *o*HC-GMC

The photocytotoxicity effect of ***o*HC-GMC** was evaluated in human lung carcinoma (A549) and human breast cancer (MCF7) cells using MTT assay (Fig. 5 and S3†). Thus, the cells were incubated with ***o*HC-GMC** at different concentrations for 1 h and then irradiated with visible light (400–700 nm, 11 mW) for 30 min, followed by further incubation for 72 h before treatment with the MTT reagent. The results showed a photo-triggered dose-dependent cell viability that decreased with the increase in concentration of the ***o*HC-GMC** prodrug (Fig. 5a). Control experiments were performed where the cells were irradiated with light or treated with ***o*HC-GMC** without light irradiation. Negligible cytotoxicity was observed in both

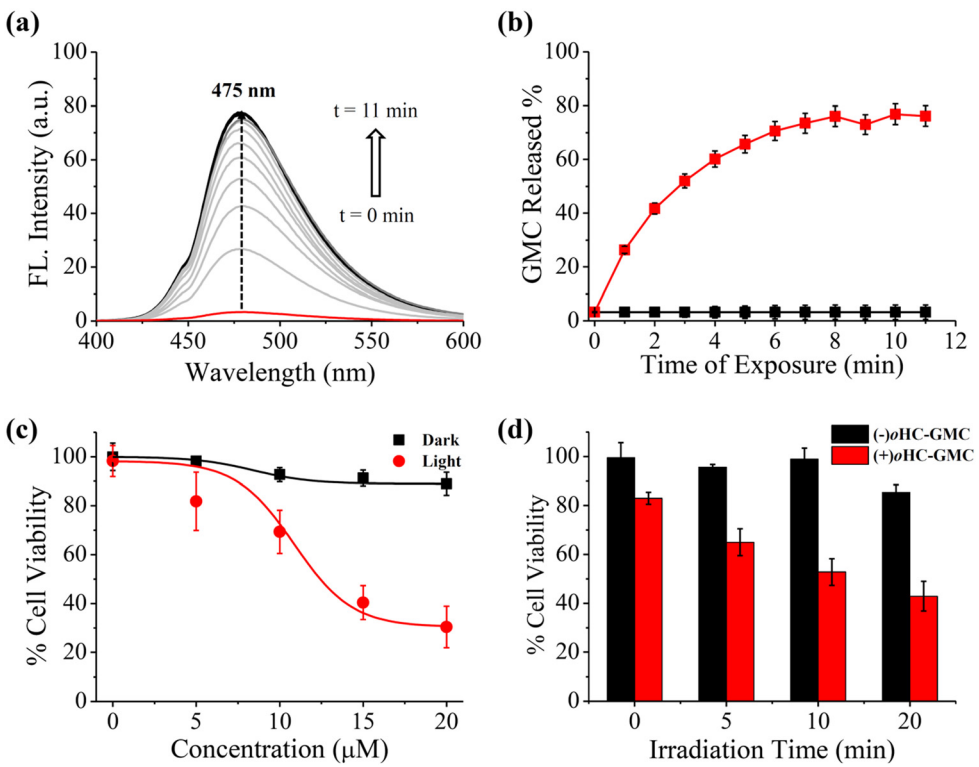


**Fig. 6** (a) Time-resolved fluorescence spectra of ***o*HC-GMC** (50 μM) in 1 : 9 DMSO/PBS (100 mM, pH 7.3) upon irradiation with two-photon NIR femtosecond laser light (800 nm, 50 mW) at 25 °C. Each time the sample was irradiated for 1 min before measuring the fluorescence spectra with an excitation wavelength of 385 nm ($\lambda_{em}$ = 475 nm). The emission spectra of ***o*HC-GMC**, before (red line) and after (black line) 11 min irradiation are highlighted. (b) Kinetics of drug release (%) from ***o*HC-GMC** (50 μM) in the dark (■) or under two-photon light (■) irradiation determined by measuring the emission ($\lambda_{em}$ = 475 nm) of coumarin product. (c) Cell viability as determined by MTT assay in A549 cells treated with different concentrations of ***o*HC-GMC** prodrug in the absence (■) or presence (●) of two-photon NIR light (800 nm, 50 mW) for 10 min of irradiation. (d) Cell viability as determined by MTT assay in A549 cells treated without (–) or with (+) the ***o*HC-GMC** prodrug (10 μM) by varying the irradiation time of two-photon NIR light (800 nm, 50 mW).

 

cases, indicating that there was no drug release from ***o*HC-GMC** in the absence of light. The $IC_{50}$ values of the ***o*HC-GMC** prodrug in A549 and MCF7 cells in visible light were determined to be 5.05 ± 0.30 μM and 5.45 ± 0.27 μM, respectively, whereas the prodrug showed negligible cytotoxicity in the dark up to the tested concentration of 20 μM (Fig. 5a and S3†). Further, the cell viability of ***o*HC-GMC** was determined by varying the exposure time to light. For this, cells were treated with prodrug (5 μM) and irradiated for different time points (0, 10, 20, and 30 min). A temporally controlled cell death was observed, wherein the cell viability decreased with increase in irradiation time (Fig. 5b). In contrast, there was no effect of light on $IC_{50}$ values of free **GMC** observed in both A549 ($IC_{50}$ = 0.65 ± 0.03 μM in light and 0.75 μM ± 0.05 in the dark) and MCF7 cells ($IC_{50}$ = 1.36 ± 0.07 μM in light and 1.46 ± 0.08 μM in the dark) (Fig. S4†). Hence, we conclude that the cytotoxicity of our prodrug can be regulated by adjusting the irradiation time period or concentration which is not possible to achieve with the free drug.

### NIR-light-triggered drug release and photocytotoxicity of *o*HC-GMC

The results of our visible-light-induced drug release and photocytotoxicity of the ***o*HC-GMC** prodrug further encouraged us to study its drug release and photocytotoxicity properties with NIR light irradiation (Fig. 6). NIR-light-triggered drug release systems are ideal in terms of clinical applications since NIR light has a far greater depth of penetration into biological tissues and less harmful effects on human tissues than visible or UV light.[47,48] Thus, the solution of ***o*HC-GMC** was irradiated with two-photon NIR light (800 nm, 50 mW) from a femtosecond laser and the drug release properties were monitored by absorption and fluorescence spectroscopy (Fig. 6a and b and S5†). Interestingly, our ***o*HC-GMC** prodrug showed efficient drug release, which was determined to be 77% by fluorescence spectroscopy, upon irradiation with NIR light for 11 min. This result is remarkable and better than that of a previously reported *o*HC-based system which demonstrated only 32% drug release after 22 min of NIR light irradiation.[37] We have also determined the two-photon uncaging cross section ($\delta_u$) for *E*-to-*Z* photoisomerization of ***o*HC-GMC** with two-photon excitation at 800 nm using the formula $\delta_u = \Phi_u^{(2)} \times \varepsilon^{(2)}$. The $\delta_u$ value of our system was found to be 1.6 GM at 800 nm (1 GM = $10^{-50}$ $cm^4$ s per photon), which is an order of magnitude larger than the 0.1 GM limit that was cited as a key factor for successful use in biological systems (Table S1†). The $\delta_u$ value of our caged system is similar to that of other *o*HC-based systems reported in the literature.[25,33,35] Hence, the uncaging cross section of ***o*HC-GMC** suggested its suitability for biological application.

Next, we evaluated the photocytotoxicity effect of ***o*HC-GMC** on cancer cells irradiated with two-photon NIR light by MTT assay (Fig. 6c and d). Accordingly, A549 cells treated with different concentrations of ***o*HC-GMC** were incubated for 1 h and then exposed to two-photon NIR light (800 nm, 50 mW) for 10 min, followed by further incubation for 72 h before MTT addition. Interestingly, our prodrug also showed good photocytotoxicity under NIR light to A549 cells with an $IC_{50}$ value of 12.52 ± 0.62 μM, while no cytotoxicity was observed in the dark (Fig. 6c). On the other hand, there was no difference in the cytotoxicity of **GMC** observed in the dark ($IC_{50}$ = 0.75 ± 0.05 μM) and under NIR light ($IC_{50}$ = 0.80 ± 0.04 μM) to A549 cells (Fig. S6†). Further, the cell viability of ***o*HC-GMC** (10 μM) was determined by varying the irradiation time points (0, 5, 10, and 20 min) in NIR light (Fig. 6d). A temporally controlled cell death was observed and the cell viability decreased with the increase in two-photon NIR light irradiation time, which was found to be 35%, 47%, and 57% at 5, 10, and 20 min, respectively, whereas minimal cytotoxicity was determined with the cells irradiated with NIR light without treatment with ***o*HC-GMC**. Again, the cell death by our prodrug with NIR light is higher than that reported in the *o*HC-based system.[37] Hence our ***o*HC-GMC** prodrug is a promising system demonstrating NIR-triggered temporally controlled efficient drug release and significant photocytotoxicity activity which could be useful for potential therapeutic applications in medicinal chemistry.

## Conclusions

In conclusion, we have reported a photoactivatable prodrug (***o*HC-GMC**) which showed on-demand, temporally controlled, and efficient drug release with real-time monitoring and photocytotoxicity activity under both visible (one-photon) and NIR (two-photon) light. The prodrug efficiently releases drug upon irradiation with visible light for 20 min, resulting in 89% drug release. Furthermore, the efficient drug release (77%) by the prodrug was determined by irradiation with NIR light for just 11 min which is better than that of other reported *o*HC-based systems. Moreover, the drug release can be monitored by the formation of the strongly fluorescent by-product coumarin reporter. The prodrug targets mitochondria without its functionalization to a mitochondria-targeting moiety, which was determined by FACS analysis and fluorescence microscopy imaging. The ***o*HC-GMC** showed light-triggered, dose-dependent, and temporally controlled cell death, whereas negligible cell death was observed in the absence of light. In contrast, no effect of light on the cytotoxicity of free **GMC** was observed. Our developed photoactivatable ***o*HC-GMC** prodrug system is superior to other *o*HC-based systems in literature reports in both the context of drug release and photocytotoxicity by either visible or NIR light irradiation. We envision that this type of photoactivatable system could be useful and in the future could find its application for developing advanced therapy.

# Experimental section

## Materials

Toluene, MeCN, EtOH, DMF and DMSO were used as HPLC grade without further drying. 4-(Diethylamino)-2-hydroxybenzaldehyde, carboethoxymethylidenetriphenylphosphorane, diisopropylethyl amine (DIPEA), sodium phosphate dibasic and sodium phosphate monobasic were purchased from Alfa-Aesar. Pyridine, Mito Red dye, and 5,5′,6,6′-tetrachloro-1,1′,3,3′-tetraethylbenzimidazolylcarbocyanine iodide (JC-1) were obtained from Sigma-Aldrich, and 1-ethyl-3-(3-dimethylaminopropyl) carbodiimide (EDC) and 1-hydroxybenzotriazole hydrate (HOBt) were sourced from SRL. Gemcitabine hydrochloride was purchased from TCI Chemicals (India) Pvt. Ltd and sodium hydroxide was obtained from Central Drug House (CDH). Trypsin, Dulbecco's modified Eagle's medium (DMEM), fetal bovine serum (FBS), 3-(4,5-dimethylthiazol-2-yl)-2,5-diphenyltetrazolium bromide (MTT), Dulbecco's phosphate-buffered saline (PBS), penicillin–streptomycin solution (pen-strep), and 35 mm glass bottom plates were procured from Thermo Fischer Scientific. A thin-layer chromatograph (TLC) system was sourced from Merck, Germany. A visible light source (LED lamp, 400–700 nm, 15 W) was procured from Philips, India. The purity of compounds **1** and **2** was found to be ≥95% by NMR and high-resolution mass spectra, while the purity of the final compound (***o*HC-GMC**) utilized for biological evaluation was determined to be ≥95% by NMR, high-resolution mass spectra and RP-HPLC.

## Synthesis and characterization

**Synthesis of compound 1.** 4-(Diethylamino)-2-hydroxybenzaldehyde (50 mg, 0.26 mmol, 1 eq.) and carboethoxymethylidenetriphenylphosphorane (135.2 mg, 0.39 mmol, 1.5 eq.) in 1 mL of dry toluene was heated at 60 °C under an argon atmosphere in the dark for 9 h. Then, the reaction mixture was allowed to cool to room temperature, and subsequently toluene was evaporated under reduced pressure. The obtained crude product was purified by silica gel column chromatography using hexane/EtOAc (2 : 1) to afford the product as a light-yellow solid (65.5 mg, 96%).

$^1$H NMR (500 MHz, $CDCl_3$): $\delta$ (ppm) 7.94 (d, $J$ = 12.9 Hz, 1H), 7.31 (d, $J$ = 8.9 Hz, 1H), 6.37 (d, $J$ = 12.9 Hz, 1H), 6.24 (d, $J$ = 2.5 Hz, 1H), 6.08 (d, $J$ = 2.5 Hz, 1H), 4.25 (q, $J$ = 7.1 Hz, 2H), 3.34 (q, $J$ = 7.1 Hz, 4H), 1.33 (t, $J$ = 7.1 Hz, 3H), 1.16 (t, $J$ = 7.1 Hz, 6H). $^{13}$C NMR (125 MHz, $CDCl_3$): $\delta$ (ppm) 169.38, 157.46, 150.77, 141.08, 130.82, 111.86, 109.69, 104.99, 98.13, 60.23, 44.60, 14.57, 12.78. ESI-MS ($m/z$): calculated 264.1600 $[M + H]^+$, found 264.1608.

**Synthesis of compound 2.** Compound **1** (65.5 mg, 0.25 mmol, 1 eq.) was dissolved in 2 mL of EtOH and 1.2 mL of 2 M NaOH and stirred at 50 °C in the dark for 24 h. Then the reaction mixture was cooled to RT and diluted with EtOAc. The reaction mixture was acidified with 1.0 M HCl to keep a pH of 1 to 3. The aqueous phase was extracted with EtOAc (3 × 20 mL). The combined organic phase was further washed with brine (25 mL), dried over anhydrous $MgSO_4$, filtered and evaporated to achieve the product as a yellow solid (43.8 mg, 74%).

$^1$H NMR (500 MHz, DMSO-$d_6$): $\delta$ (ppm) 11.72 (s, 1H), 9.79 (s, 1H), 7.68 (d, $J$ = 11.9 Hz, 1H), 7.32 (d, $J$ = 8.8 Hz, 1H), 6.18 (d, $J$ = 11.1 Hz, 2H), 6.14 (s, 1H), 3.31 (q, $J$ = 7.0 Hz, 4H), 1.09 (t, $J$ = 6.8 Hz, 6H). $^{13}$C NMR (125 MHz, DMSO-$d_6$): $\delta$ (ppm) 168.87, 158.43, 150.26, 140.45, 130.19, 111.14, 108.82, 103.91, 97.34, 43.87, 12.59. ESI-MS ($m/z$): calculated 274.0846 $[M + K]^+$, found 274.0945.

**Synthesis of *o*HC-GMC.** Compound **2** (17.2 mg, 0.074 mmol, 1.1 eq.), EDC (16.6 mg, 0.086 mmol, 1.3 eq.), HOBt (12.4 mg, 0.8 mmol, 1.2 eq.) and pyridine (10 μL, 0.124 mmol, 1.9 eq.) were taken in 200 μL of DMF and allowed to stir at RT for 3 h under an argon atmosphere. To the above mixture, gemcitabine hydrochloride (20 mg, 0.066 mmol, 1 eq.) and DIPEA (46.6 μL, 0.266 mmol, 4 eq.) in 200 μL of DMF were added and the mixture was continuously stirred at RT for 24 h in the dark. Then, the solvent was dried to give an oily crude product which was dissolved in DCM and washed with water. The organic fraction was dried over anhydrous $Na_2SO_4$, filtered and evaporated. The obtained yellow green powder was further purified by preparative TLC using DCM/MeOH (20 : 1) to furnish a green powder as a final product (13.2 mg, 37%).

$^1$H NMR (500 MHz, $CDCl_3$): $\delta$ (ppm) 7.89 (m, 1H), 7.72 (d, $J$ = 12.6 Hz, 1H), 7.54 (d, $J$ = 7.4 Hz, 1H), 7.23 (s, 1H), 6.82 (dd, $J$ = 7.3, 5.3 Hz, 1H), 6.30 (m, 2H), 6.04 (d, $J$ = 7.4 Hz, 1H), 5.34 (t, $J$ = 3.8 Hz, 1H), 4.28 (dd, $J$ = 7.0, 2.0 Hz, 1H), 4.20 (dd, $J$ = 5.5, 1.8 Hz, 2H), 3.34 (q, $J$ = 5.5 Hz, 4H), 1.17 (t, $J$ = 5.7 Hz, 6H). $^{13}$C NMR (125 MHz, $CDCl_3$): $\delta$ (ppm) 169.38, 161.72, 151.63, 147.49, 142.07, 141.96, 140.10, 137.15, 132.28, 132.20, 128.71, 125.53, 121.39, 118.70, 113.29, 105.45, 81.18, 70.03, 61.49, 41.70, 13.80. IR (ATR) $\nu$ ($cm^{-1}$): 3186 br, 2920 w, 1724 w (C=O), 1660 m (C=C), 1575 s (N–H), 1271 m (C–O–C), 987 m, 786 m, 688 w. ESI-MS ($m/z$): calculated 481.1899 $[M + H]^+$, found 481.1928.

## Visible-light-triggered drug release by absorption spectroscopy

The drug release by ***o*HC-GMC** upon photoirradiation was monitored by absorption spectroscopy. For this, ***o*HC-GMC** (10 μM) was dissolved in 1 : 9 DMSO/PBS (100 mM, pH 7.3) and taken in a quartz cuvette. Then the solution in the cuvette was exposed to visible light (400–700 nm, 11 mW) at a distance of 2 cm for 0–20 min. Each time, the solution was exposed to light for 2 min at 25 °C and the absorption spectra were recorded just after photoirradiation.

## Visible-light-triggered drug release by fluorescence spectroscopy

The light-triggered drug release profile of ***o*HC-GMC** was also examined by fluorescence spectroscopy. ***o*HC-GMC** (50 μM) dissolved in 1 : 9 DMSO/PBS (100 mM, pH 7.3) was irradiated with visible light (400–700 nm, 11 mW) at a distance of 2 cm for 0–20 min. The fluorescence spectra of ***o*HC-GMC** were

 

measured after each photoirradiation for 2 min at 25 °C. The drug release from ***o*HC-GMC** was monitored by recording the emission intensity of coumarin reporter ($\lambda_{ex}$ = 385 nm and $\lambda_{em}$ = 475 nm). For the dark control experiment, a similar protocol was followed without exposure of ***o*HC-GMC** to visible light.

### Visible-light-triggered drug release by HPLC

The drug release of ***o*HC-GMC** was also further monitored by HPLC. Thus, ***o*HC-GMC** (50 μM) in 1 : 9 MeCN/PBS (100 mM, pH 7.3) was taken in a quartz cuvette and irradiated with visible light (400–700 nm, 11 mW) at a distance of 2 cm at RT. After each photoirradiation, an aliquot (10 μL) was taken from the ***o*HC-GMC** solution and analyzed by RP-HPLC using MeCN/water (1 : 1) both containing 0.1% TFA in the mobile phase at a flow rate of 1.0 mL $min^{-1}$. The chromatograms were analyzed at 254 nm. The relative percentage of photoinduced conversion of ***o*HC-GMC** to **GMC** was determined by comparing their relative HPLC peak areas at each time point.

### Determination of photo-uncaging or photoconversion quantum yields[30,49]

The photo-uncaging or photoconversion quantum yield ($\Phi_u$) is defined as the probability of photoconversion after absorption of a photon or the ratio of the conversion rate ($R_p$) of the absorption rate of photons ($R_{abs}$):

$$\Phi_u = \frac{R_p}{R_{abs}} = \frac{1}{\tau_p R_{abs}} = \frac{1}{\tau_p \sigma_\lambda I_\lambda \left(\frac{\lambda}{hc}\right)}$$

where $\tau_p$ = decay constant (min) in the exponential fit of the decaying absorption values for the reactant.

$\sigma_\lambda$ = absorption cross section ($cm^2$); it is related to the molar absorption coefficient by the equation $\sigma_\lambda = (1000)2.303\varepsilon_\lambda/N_A$

$I_\lambda$ = irradiance at the sample (mW $cm^{-2}$)

$\lambda$ = irradiation wavelength (nm)

$h$ = Planck's constant

$c$ = speed of light

The photo-uncaging or photoconversion quantum yields ($\Phi_u$) were determined by monitoring the changes in absorbance values of ***o*HC-GMC** and its photoproduct coumarin compound over time. ***o*HC-GMC** (50 μM) in 1 : 9 MeCN/PBS (100 mM, pH 7.3) was taken in a quartz cuvette and irradiated with visible light (400–700 nm, 11 mW) or two-photon NIR light (800 nm, 50 mW). After each photoirradiation, an aliquot (10 μL) was taken from the ***o*HC-GMC** solution and analyzed by RP-HPLC. The formation of the photoproduct coumarin and disappearance of ***o*HC-GMC** were quantified in terms of the absorption peak area of the chromatograms. The time constant $\tau_p$ was determined from the exponential fit of the disappearance of the ***o*HC-GMC** prodrug which was used to calculate the photo-uncaging quantum yield ($\Phi_u$). The two-photon uncaging cross section ($\delta_u$) with two-photon excitation at 800 nm was determined using the formula $\delta_u = \Phi_u^{(2)} \times \varepsilon^{(2)}$.

### Cell culture

Human lung carcinoma (A549) and human breast cancer (MCF7) cells were procured from the National Center for Cell Science (NCCS) Pune. The cells were cultured in high-glucose Dulbecco's modified Eagle's medium (DMEM) containing 10% FBS and 1% penicillin–streptomycin at 37 °C in a $CO_2$ incubator (5% $CO_2$). When the cells reached 90% confluency, the cells were trypsinized, centrifuged and redispersed in complete medium. The cells were seeded in 96-well microplates (at a density of 9000 cells per well) or in glass well 35 mm μ-dishes (at a density of $2 \times 10^5$ cells per dish) and grown at 37 °C for 24 h in a 5% $CO_2$ incubator.

### Cellular uptake

A549 cells were seeded in 6 well plates at a density of $1.5 \times 10^5$ cells per well. The cells were washed twice with PBS and incubated with 10 μM ***o*HC-GMC** (prepared in complete culture medium containing 1% DMSO) for 0, 0.5, 1 and 2 h at 37 °C. Following incubation, the medium was removed and replaced with 200 μL of PBS and irradiated with visible light (400–700 nm, 11 mW) for 10 min. After irradiation the cells were again washed with PBS followed by trypsinization and resuspended in 500 μL of HBSS (Hanks' balanced salt solution). Then the blue fluorescence of the photoproduct (*i.e.*, coumarin reporter) of ***o*HC-GMC** in A549 cells was determined using a flow cytometer (FACS-LSR Fortessa; BD Biosciences, USA). Approximately 10 000 cells were counted for each sample and BD FACS-DIVA Software was used to obtain the cells for each measurement. The analysis was done using FlowJo software (Tree Star).

### Cellular imaging with real-time monitoring of drug release

The intracellular drug release was determined by recording the intracellular blue fluorescence intensity of the formed coumarin reporter upon photoirradiation of ***o*HC-GMC** inside the cells. For this, A549 cells were seeded in a 12-well culture plate at a density of $2 \times 10^5$ cells per well one day prior to the experiments. Then the cells were treated with ***o*HC-GMC** (10 μM) and incubated for 1 h at 37 °C in the dark. After that, the medium was removed from the wells and the cells were washed with cold PBS (2 × 2 mL) followed by irradiation with visible light (400–700 nm, 11 mW) for different time periods (0, 2, 5, 10, 15, 20, and 30 min). Further, the cells were incubated for 10 min before performing microscopy imaging using an inverted fluorescence microscope (Olympus IX70, Tokyo, Japan) equipped with a digital camera (DP71, Olympus). The fluorescence was analyzed using the blue channel. The increase in fluorescence intensity due to the release of drug was evaluated with ImageJ and is given as a mean value of 30 cells. Data points were fitted to an exponential equation.

### Subcellular release

The subcellular release of the photoproduct coumarin reporter of ***o*HC-GMC** in the intracellular medium was determined by fluorescence microscopy. Accordingly, A549 cells were seeded in 35 mm 6 well plates at a density of $2.5 \times 10^5$ cells per well one day prior to the experiments. The cells were incubated with ***o*HC-GMC** (10 μM) in DMEM complete medium for 1 h at 37 °C. Then the cells were washed with PBS which was replaced with 1 mL PBS before irradiation with visible light (400–700 nm, 11 mW) for 10 min. Following light irradiation, PBS was replaced with medium and then incubated with Mito Red (100 nM) for 15 min. The medium was then removed and the cells were washed thoroughly with PBS (3 × 2 mL) before microscopy imaging was performed using an inverted fluorescence microscope (Olympus IX70, Tokyo, Japan) equipped with a digital camera (DP71, Olympus). The fluorescence of the photoproduct coumarin reporter was analyzed with a DAPI filter ($\lambda_{ex}/\lambda_{em}$ = 350/460 nm), and the Mito Red fluorescence was analyzed with a TRITC filter set ($\lambda_{ex}/\lambda_{em}$ = 550/580 nm). The extent of co-localization was calculated by a scatter plot using Pearson's correlation coefficient (PCC).

### Mitochondrial accumulation of *o*HC-GMC

Mitochondrial accumulation of ***o*HC-GMC** was assessed by monitoring the change in MMP ($\Delta\Psi_m$) using JC-1 dye. JC-1 dye tends to aggregate in healthy mitochondria and exhibits red fluorescence,[41] whereas in depolarized mitochondria, this dye accumulates in the cytoplasm and emits green fluorescence. Thus, the loss of $\Delta\Psi_m$ can be determined in healthy (polarized) and unhealthy (depolarized) cells by measuring the ratio of red-to-green fluorescence of JC-1. Hence, A549 cells at a density of $1.5 \times 10^5$ cells were seeded in 35 mm dishes. After 24 h, the cells were treated with ***o*HC-GMC** (10 μM) for 30 min and 1 h. Post-treatment, the cells were washed twice with 1× PBS. The cells were then trypsinized and harvested by centrifugation at 400*g* for 15 min at RT. To each cell pellet, 0.5 mL of freshly prepared JC-1 (5 μg $mL^{-1}$) working solution was added. The cells were gently resuspended by pipetting the solution, incubated at 37 °C in a $CO_2$ incubator for 15 min. The cells were then washed twice with 1× assay buffer and finally resuspended in 500 μL of 1× assay buffer for measurement. JC-1 was excited at 488 nm and emission was monitored at 515–545 nm (green) and 570–600 nm (red) using BD FACS Aria immediately after staining. 10 000 events were acquired for each sample. The analysis was done using FlowJo software (Tree Star, USA).

### Photocytotoxicity assay under visible light

The photocytotoxicity activity of ***o*HC-GMC** in A549 and MCF7 cells was evaluated under visible light (400–700 nm, 11 mW) by MTT assays. For this, different concentrations of ***o*HC-GMC** and **GMC** were prepared in complete culture medium containing ≤1% DMSO. The cells were cultured at a density of 9000 cells per well in 96 well cell culture plates with DMEM (200 μL) and incubated at 37 °C for 24 h. Then, the medium in the 96 well cell cultured plates was removed and replaced with 200 μL of medium containing different concentrations of ***o*HC-GMC** or **GMC** and incubated for 1 h at 37 °C in a $CO_2$ incubator in the dark. After that the medium was removed and the cells were washed twice with PBS and replaced with 200 μL of PBS. Next, the cells were irradiated with or without visible light for 10, 20, and 30 min. Following irradiation, the PBS was replaced with 200 μL of complete medium and then further incubated in the dark for 72 h. Subsequently, the cells were washed with PBS followed by addition of 200 μL of DMEM and 20 μL of MTT solution (5 mg $mL^{-1}$ in PBS) to each well and incubated at 37 °C for 2 h. Then the medium was discarded and replaced with 200 μL of DMSO in each well to dissolve the formazan crystals formed. The cell viability was determined by measuring the absorbance at 570 nm using a SpectraMax M2 microtitre plate reader (Molecular Devices LLC, USA). For the dark control set, a similar procedure was followed without exposure of ***o*HC-GMC** or **GMC** to visible light. The data obtained were analysed with Origin Pro 8.5 software.

### NIR-triggered drug release by absorption spectroscopy

The drug release from ***o*HC-GMC** upon photoirradiation with two-photon light (excitation at 800 nm, average power ~50 mW) for 0–20 min was monitored by absorption spectroscopy. For this, a 10 μM solution of ***o*HC-GMC** in 1 : 9 DMSO/PBS (100 mM, pH 7.3) was taken in a quartz cuvette and exposed to NIR light each time before measuring the absorption spectra. While irradiating the sample, we ensured maximum exposure of the sample to the laser light by making light pass through the solution from the top.

### NIR-triggered drug release by fluorescence spectroscopy

The NIR-triggered drug release was examined by irradiation with two-photon light (excitation at 800 nm, average power ~50 mW) from a femtosecond laser as described in the literature.[37] Briefly, ***o*HC-GMC** (50 μM) solution in 1 : 9 DMSO/PBS (100 mM, pH 7.3) was irradiated with two-photon light (800 nm, 50 mW) for 0–11 min. Here again, during sample irradiation, we ensured maximum exposure of the sample to the laser light by making light pass through the solution from the top. Each time, the sample solution was irradiated for 1 min before measuring the fluorescence spectra using an Edinburgh Instruments F900 spectrophotometer. The drug release by ***o*HC-GMC** was monitored by measuring the emission intensity of coumarin reporter ($\lambda_{ex}$ = 385 nm and $\lambda_{em}$ = 475 nm). For the dark control set, a similar procedure was followed without exposure of ***o*HC-GMC** to two-photon light.

### Photocytotoxicity assay under NIR light

The photocytotoxicity experiments with NIR light followed a similar protocol to that described in the section Photocytotoxicity assay under visible light. Briefly, the

 

cultured A549 cells (9000 cells per well) in 96 well plates containing 100 μL DMEM were treated with different concentrations of ***o*HC-GMC** or **GMC** and incubated for 1 h at 37 °C in a $CO_2$ incubator in the dark. Then the medium was removed from the cultured plates and replaced with 200 μL of PBS. Subsequently, the cells were irradiated with NIR femtosecond laser light using two-photon excitation at 800 nm (50 mW) for 0, 5, 10, 15, and 20 min. After photoexposure, the PBS was removed and replaced with 200 μL of medium, and the cells were further incubated for 72 h in the dark. Next, the cells were washed with PBS followed by addition of 200 μL of fresh culture medium and 20 μL of MTT solution (5 mg $mL^{-1}$ in PBS) to each well and incubated for 2 h. The medium was then discarded and 200 μL of DMSO was added to each well to dissolve the formazan crystals formed by the living cells. The cell viability was determined by measuring the absorbance at 570 nm. For the dark control experiment, a similar protocol was followed without exposure of ***o*HC-GMC** or **GMC** to NIR light. The results were analysed using the Origin Pro 8.5 software.

## Author contributions

P. K. S. conceptualized the project, designed the experiments, and wrote and edited the manuscript. Aj. G. synthesized and characterized the compounds and performed the experiments in extracellular and intracellular medium, analyzed the experimental data, and wrote the manuscript. N. S. assisted in synthesis and characterization of compounds and drug release studies in extracellular medium. Ar. G. assisted in synthesis of compounds and two-photon NIR experiment. N. D. helped in performing experiments under two-photon NIR light. S. K. edited the manuscript.

## Conflicts of interest

There are no conflicts to declare.

## Acknowledgements

P. K. S. acknowledges MHRD-STARS (Project Code: MoE-STARS/STARS-1/374) for financial support. We thank AIRF, JNU, for the instrumentation facilities. Aj. G. gratefully acknowledges MHRD-STARS for a fellowship. Ar. G. acknowledges UGC for a fellowship. We thank Prof. P. K. Chowdhury, IIT Delhi, for generously allowing us to use the spectrofluorometer and absorption spectrophotometer. The authors would also like to thank M. K. Gupta, Amity University, Noida, for the help in FACS data collection.

## References

1 C. Brieke, F. Rohrbach, A. Gottschalk, G. Mayer and A. Heckel, *Angew. Chem., Int. Ed.*, 2012, **51**, 8446–8476.
2 N. Ankenbruck, T. Courtney, Y. Naro and A. Deiters, *Angew. Chem., Int. Ed.*, 2017, **57**, 2768–2798.
3 B. M. Vickerman, E. M. Zywot, T. K. Tarrant and D. S. Lawrence, *Nat. Rev. Chem.*, 2021, **5**, 816–834.
4 L. Kowalik and J. K. Chen, *Nat. Chem. Biol.*, 2017, **13**, 587–598.
5 I. Elamri, C. Abdellaoui, J. K. Bains, K. F. Hohmann, S. L. Gande, E. Stirnal, J. Wachtveitl and H. Schwalbe, *J. Am. Chem. Soc.*, 2021, **143**, 10596–10603.
6 J. E. T. Corrie, T. Furuta, R. S. Givens, A. L. Yousef and M. Goeldner, *Photoremovable Protecting Groups Used for the Caging of Biomolecules*, WILEY-VCH, Weinheim, 2005.
7 A. P. Pelliccioli and J. Wirz, *Photochem. Photobiol. Sci.*, 2002, **1**, 441–458.
8 P. Klán, T. Šolomek, C. G. Bochet, A. Blanc, R. Givens, M. Rubina, V. Popik, A. Kostikov and J. Wirz, *Chem. Rev.*, 2013, **113**, 119–191.
9 C. G. Bochet, *J. Chem. Soc., Perkin Trans. 1*, 2002, **2**, 125–142.
10 R. Weinstain, T. Slanina, D. Kand and P. Klán, *Chem. Rev.*, 2020, **120**, 13135–13272.
11 A. Bardhan and A. Deiters, *Curr. Opin. Struct. Biol.*, 2019, **57**, 164–175.
12 I. Aujard, C. Benbrahim, M. Gouget, O. Ruel, J.-B. Baudin, P. Neveu and L. Jullien, *Chem. – Eur. J.*, 2006, **12**, 6865–6879.
13 S. Shah, P. K. Sasmal and K. B. Lee, *J. Mater. Chem. B*, 2014, **2**, 7685–7693.
14 E. Procházková, P. Šimon, M. Straka, J. Filo, M. Majek, M. Cigáň and O. Baszczyňski, *Chem. Commun.*, 2021, **57**, 211–214.
15 T. Furuta, S. S. Wang, J. L. Dantzker, T. M. Dore, W. J. Bybee, E. M. Callaway, W. Denk and R. Y. Tsien, *Proc. Natl. Acad. Sci. U. S. A.*, 1999, **96**, 1193–1200.
16 M. Bojtár, A. Kormos, K. Kis-Petik, M. Kellermayer and P. Kele, *Org. Lett.*, 2019, **21**, 9410–9414.
17 M. López-Corrales, A. Rovira, A. Gandioso, M. Bosch, S. Nonell and V. Marchán, *Chem. – Eur. J.*, 2020, **26**, 16222–16227.
18 L. A. Wells, M. A. Brook and H. Sheardown, *Macromol. Biosci.*, 2011, **11**, 988–998.
19 K. A. Günay, T. L. Ceccato, J. S. Silver, K. L. Bannister, O. J. Bednarski, L. A. Leinwand and K. S. Anseth, *Angew. Chem., Int. Ed.*, 2019, **58**, 9912–9916.
20 N. Asad, D. Deodato, X. Lan, M. B. Widegren, D. L. Phillips, L. Du and T. M. Dore, *J. Am. Chem. Soc.*, 2017, **139**, 12591–12600.
21 A.-L. K. Hennig, D. Deodato, N. Asad, C. Herbivo and T. M. Dore, *J. Org. Chem.*, 2020, **85**, 726–744.
22 A. K. Singh, M. Kundu, S. Roy, B. Roy, S. S. Shah, A. V. Nair, B. Pal, M. Mondal and N. D. P. Singh, *Chem. Commun.*, 2020, **56**, 9986–9989.
23 A. Gupta, A. Gautam and P. K. Sasmal, *J. Med. Chem.*, 2022, **65**, 5274–5287.
24 A. D. Turner, S. V. Pizzo, G. W. Rozakis and N. A. Porter, *J. Am. Chem. Soc.*, 1987, **109**, 1274–1275.
25 N. Gagey, P. Neveu and L. Jullien, *Angew. Chem., Int. Ed.*, 2007, **46**, 2467–2469.
26 A. Paul, R. Mengji, O. A. Chandy, S. Nandi, M. Bera, A. Jana, A. Anoop and N. D. P. Singh, *Org. Biomol. Chem.*, 2017, **15**, 8544–8552.

27 A. Abramov, B. Maiti, I. Keridou, J. Puiggalí, O. Reiser and D. D. Díaz, *Macromol. Rapid Commun.*, 2021, **42**, 2100213.

28 A. Paul, R. Mengji, M. Bera, M. Ojha, A. Jana and N. D. P. Singh, *Chem. Commun.*, 2020, **56**, 8412–8415.

29 R. R. Nani, A. P. Gorka, T. Nagaya, T. Yamamoto, J. Ivanic, H. Kobayashi and M. Schnermann, *ACS Cent. Sci.*, 2017, **3**, 329–337.

30 Y. Jang, T.-I. Kim, H. Kim, Y. Choi and Y. Kim, *ACS Appl. Bio Mater.*, 2019, **2**, 2567–2572.

31 A. D. Turner, S. V. Pizzo, G. Rozakis and N. A. Porter, *J. Am. Chem. Soc.*, 1988, **110**, 244–250.

32 P. B. Jones and N. A. Porter, *J. Am. Chem. Soc.*, 1999, **121**, 2753–2761.

33 N. Gagey, P. Neveu, C. Benbrahim, B. Goetz, I. Aujard, J. B. Baudin and L. Jullien, *J. Am. Chem. Soc.*, 2007, **129**, 9986–9998.

34 N. Gagey, M. Emond, P. Neveu, C. Benbrahim, B. Goetz, I. Aujard, J.-B. Baudin and L. Jullien, *Org. Lett.*, 2008, **10**, 2341–2344.

35 Y. Venkatesh, H. K. Srivastava, S. Bhattacharya, M. Mehra, P. K. Datta, S. Bandyopadhyay and N. D. P. Singh, *Org. Lett.*, 2018, **20**, 2241–2244.

36 W. Feng, C. Gao, W. Liu, H. Ren, C. Wang, K. Ge, S. Li, G. Zhou, H. Li, S. Wang, G. Jia, Z. Li and J. Zhang, *Chem. Commun.*, 2016, **52**, 9434–9437.

37 Key reference:N. Singh, A. Gupta, P. Prasad, R. K. Sah, A. Singh, S. Kumar, S. Singh, S. Gupta and P. K. Sasmal, *J. Med. Chem.*, 2021, **64**, 17813–17823.

38 A. Gupta, P. Prasad, S. Gupta and P. K. Sasmal, *ACS Appl. Mater. Interfaces*, 2020, **12**, 35967–35976.

39 D. Guo, T. Chen, D. Ye, J. Xu, H. Jiang, K. Chen, H. Wang and H. Liu, *Org. Lett.*, 2011, **11**, 2884–2887.

40 R. J. Holmila, S. A. Vance, X. Chen, H. Wu, K. Shukla, M. S. Bharadwaj, J. Mims, Z. Wary, G. Marrs, R. Singh, A. J. Molina, L. B. Poole, S. B. King and C. M. Furdui, *Sci. Rep.*, 2018, **8**, 6635.

41 S. T. Smiley, M. Reers, C. Mottola-Hartshorn, L. Mei, A. Chen, T. W. Smith, G. D. Steele and A. L. B. Chen, *Proc. Natl. Acad. Sci. U. S. A.*, 1991, **88**, 3671–3675.

42 J. Jose, A. Loudet, Y. Ueno, R. Barhoumi, R. C. Burghardt and K. Burgess, *Org. Biomol. Chem.*, 2010, **8**, 2052–2059.

43 M.-C. Frantz and P. Wipf, *Environ. Mol. Mutagen.*, 2010, **51**, 462–475.

44 M. Catalán, I. Olmedo, J. Faúndez and J. A. Jara, *Int. J. Mol. Sci.*, 2020, **21**, 8684.

45 D. C. Chan, *Cell*, 2006, **125**, 1241–1252.

46 P. Wang, J. H. Song, D. K. Song, J. Zhang and C. Hao, *Cell. Signalling*, 2006, **18**, 1528–1535.

47 J. M. Dabrowski and L. G. Arnaut, *Photochem. Photobiol. Sci.*, 2015, **14**, 1765–1780.

48 C. Ash, M. Dubec, K. Donne and T. Bashford, *Lasers Med. Sci.*, 2017, **32**, 1909–1918.

49 S. J. Lord, N. R. Conley, H.-I. D. Lee, R. Samuel, N. Liu, R. J. Twieg and W. E. Moerner, *J. Am. Chem. Soc.*, 2008, **130**, 9204–9205.